EFFICIENT SENSITIVITY CALCULATION FOR ROBUST OPTIMAL CONTROL

T. Akman[1], B. Hosseini[1], J. Diepolder[1], B. Grüter[1], R. J. M. Afonso[1,2], M. Gerdts[3], F. Holzapfel[1]
[1]Institute of Flight System Dynamics, Technical University of Munich, 85748 Garching, Germany
[2]Electronic Engineering Division, Instituto Tecnológico de Aeronáutica, 12228-900 São José dos Campos, Brazil
[3]Department of Aerospace Engineering, Universität der Bundeswehr München, 85577 Neubiberg, Germany

Abstract

Due to model and measurement uncertainties, simulation outputs of dynamic systems might not be exact and also subject to uncertainties. Especially in reentry missions unforeseen perturbations and the resulting change of the vehicle's behaviour are critical due to high velocities and heat loads. Here, trajectory planning considering uncertainties is of high interest. Therefore, it is important to quantify and reduce the dependency of the system output with respect to uncertainties. In general, reentry trajectories can be calculated by optimal control methods, giving rise to controls such that a certain cost function, e.g. the heat load, is minimized. In this study sensitivities are calculated and minimized in a multi-objective cost function in order to reduce the dependencies of the system regarding uncertain parameters. Two different sensitivity approaches, namely the forward sensitivity and adjoint method are compared. For each of the methods two discretization schemes, first the collocation and second the shooting method, are investigated.

Keywords

Robust Optimal Control, Forward Sensitivity, Backward Sensitivity, Adjoint, Sensitivity Penalty, Heat Minimal Reentry

NOMENCLATURE

$\mathbf{f}$	System dynamics
$\mathbf{f}_\lambda$	Dynamics for adjoint equation
h	Altitude
n_p	Number of parameters
n_t	Number of time steps
n_u	Number of controls
n_x	Number of states
$\mathbf{p}$	Parameters
q	Heat load at stagnation point
$\mathbf{S}$	Sensitivity matrix
t_0	Initial time
t_f	Final time
$\mathbf{u}$	Controls
V	Velocity
$\mathbf{x}$	States
$\mathbf{z}$	Optimization vector
α	Angle of attack
γ	Flight path angle
$\boldsymbol{\lambda}$	Adjoint matrix
μ	Bank angle

1. INTRODUCTION

During reentry, the vehicle's velocity is reduced from hypersonic to subsonic speed. In order to reach this high reduction of velocity, the reentry vehicle uses the effect of air resistance. By this, high heat flux acts on the vehicle resulting in high heat loads. This is safety critical for different reasons. High temperatures in either the cabin, tank or other sensitive parts of the system are critical for passengers or other flight systems in its surrounding. Furthermore, high temperature impact shortens the vehicle's lifespan and reduces reusability for further missions. By optimal control methods [1, 2] optimal flight paths can be calculated such that the heat load on the vehicle is minimal. Here, constraints that include the vehicle's dynamic behaviour, configuration, and mission specifications are considered. Therefore, mathematical models are required. Since for the modelling of the vehicle and the environment not every parameter is well known, the aforementioned optimal trajectory varies with parameter perturbations and does not meet the defined requirements. Uncertain parameter might be air density [3] or the capsule's position which might differ from the onboard estimated position [4].

©2020

doi:10.25967/490248

In robust optimal control, these parameter uncertainties are included into an optimal control problem either probabilistically [5, 6] or deterministically [7, 8]. The aim is to calculate a trajectory, that is optimal but not prone to parameter perturbations, i.e. under parameter perturbations the trajectories or some performance value should not differ significantly. The optimal solution, where no uncertainties are considered, is called *nominal solution*. The solution of the optimal control problem, where uncertainties are considered is called *robust solution*. Robust reentry trajectories under atmospheric uncertainties are studied e.g. in [9] with a differential game method or in [10] by a multiple optimization approach with perturbed air density to study the distribution of the resulting trajectories. Another robust optimal control method is minimizing sensitivities of the system output regarding uncertain parameters. The method of sensitivity minimization is presented and applied in [8, 11]. Here, the state system is augmented by the sensitivities. Hence, the discretization method used for the states is also used for the sensitivities. For large problem sizes, this might lead to high computational effort. Therefore, in [12] a hybrid method where the states are fully discretized and sensitivities are discretized using a shooting method is presented. As discussed in [13], for a large number of parameters the adjoint method might be more suitable for efficiency reasons. Therefore, in [14] adjoints instead of sensitivities are applied in order to determine gradients in optimal control problems. However, to the best knowledge of the authors, adjoints have not been applied for sensitivity minimization.

In this paper, a reentry trajectory of an Apollo capsule is robustified by minimizing the sensitivity of the final velocity with respect to the initial altitude and flight path angle. The sensitivity is incorporated into the cost function as a penalty resulting in a multi-objective optimal control problem. Two methods, the forward sensitivity and adjoint method, are applied for sensitivity calculation and compared regarding efficiency. For each method, two different discretization methods for the forward sensitivities and adjoints, namely a full discretization (analogous to the system states) and a shooting method are implemented and compared regarding efficiency. In section 2, an overview of applied optimal control theory is given. Theoretical background on the forward sensitivity and adjoint method is presented in section 3. The modelling for the dynamic system, aerodynamics, atmosphere and thermodynamics is given in section 4. In section 5 nominal and robust optimization results are presented and compared. A conclusion and outlook is given in section 6.

2. APPLIED OPTIMAL CONTROL

The aim of optimal control is to control a dynamic system such that a cost function is minimized. Mathematically, the optimization problem is stated as follows:

$$\min_{\mathbf{x},\mathbf{u}} e(\mathbf{x}(t_0),\mathbf{x}(t_f)) + g(\mathbf{S}(t_f;\mathbf{p})) \tag{1}$$

subject to the dynamic constraints

$$\dot{\mathbf{x}}(t) = \mathbf{f}(\mathbf{x}(t),\mathbf{u}(t);\mathbf{p}) \tag{2}$$

with $\mathbf{f}\colon \mathbb{R}^{n_x} \times \mathbb{R}^{n_u} \times \mathbb{R}^{n_p} \to \mathbb{R}^{n_x}$, the inequality constraints

$$\mathbf{c}_{ineq}(\mathbf{x}(t),\mathbf{u}(t);\mathbf{p}) \leq 0 \tag{3}$$

for all $t \in [t_0, t_f]$ with $\mathbf{c}_{ineq}\colon \mathbb{R}^{n_x} \times \mathbb{R}^{n_u} \times \mathbb{R}^{n_p} \to \mathbb{R}^{n_{ineq}}$ and the initial and final boundary conditions

$$\boldsymbol{\psi}(\mathbf{x}(t_0),\mathbf{x}(t_f)) = 0 \tag{4}$$

with $\boldsymbol{\psi}\colon \mathbb{R}^{n_x} \times \mathbb{R}^{n_x} \to \mathbb{R}^{n_\psi}$. Here, e represents the Mayer cost function, $\mathbf{x}\colon \mathbb{R} \to \mathbb{R}^{n_x}$ the state history, $\mathbf{u}\colon \mathbb{R} \to \mathbb{R}^{n_u}$ the control history and $\mathbf{p} \in \mathbb{R}^{n_p}$ the parameter vector. Furthermore, $\mathbf{S}(t_f;\mathbf{p})$ denotes the sensitivity $\mathbf{S}(t_f) = \frac{\partial \mathbf{x}(t_f)}{\partial \mathbf{p}}$ of the states regarding the parameters $\mathbf{p}$ and $g\colon \mathbb{R}^{n_x} \times \mathbb{R}^{n_p} \to \mathbb{R}$ denotes a nonlinear function applied to the aforementioned sensitivity, e.g. a suitable norm. This term is introduced in the robust optimal control approach, where sensitivities are minimized to robustify the resulting trajectory and reduce variations of the trajectory when the parameters $\mathbf{p}$ are perturbed. This approach is introduced in section 3. Please note that the Mayer cost formulation can include, without loss of generality, Lagrange cost functions by introducing new states accordingly.

There are two main approaches to solve an optimal control problem. In function space methods, optimality conditions for the infinite dimensional optimal control problem are formulated and then discretized. In the discretization approach, the problem is first discretized on a time grid, thereby transcribed to a parametric optimization problem and then solved with methods for finite dimensional optimization problems as applied in this paper. [1, 2]

In the present study, the optimal control tool FALCON.m [15] is used. We apply full discretization on the continuous problem. Here, every state and control at every discretized point of time is included into the optimization vector. Hence, the optimization vector $\mathbf{z}$ takes the form

$$\begin{aligned}\mathbf{z} =& [x_1(t_0),\dots,x_{n_x}(t_0),u_1(t_0),\dots,u_{n_u}(t_0),\\ &\dots,x_1(t_f),\dots,x_{n_x}(t_f),u_1(t_f),\dots,u_{n_u}(t_f)]^T.\end{aligned} \tag{5}$$

©2020

In order to fulfill the dynamic constraints, the system is simulated by one step at each discretized point. The discrepancy between the simulated and the optimized states is then constrained to be zero in the so called defect constraints [1]. Therefore, no integration of the system over the whole time interval is required.
In contrast, in the single shooting method, only the controls are fully discretized and fully included into the optimization vector. From the states, only the initial state is contained in the optimization vector. The remaining state values are calculated by one integration sweep. Therewith, the system dynamics are fulfilled such that no introduction of integration defect constraints is required. [1, 2] Due to the decoupled integration of the states the collocation method gives rise to a sparse problem but requires the introduction of defect constraints [1, 16]. On the other hand, the single shooting method does not increase problem size significantly, but has the drawback of a dense problem structure. Therefore, to incorporate the sensitivities from section 3 into an optimal control problem, both a pure collocation method collocating states and forward sensitivities/adjoints respectively and a hybrid method collocating states and shooting forward sensitivities/adjoints are applied and compared.

3. FORWARD AND BACKWARD SENSITIVITY

In this section, two methods to calculate the sensitivity of a state with respect to a parameter are presented, namely the forward sensitivity and the adjoint method. Let x_k be the k-th state with $k \in \{1, \dots, n_x\}$. The aim is to calculate the dependency of the final state $x_k(t_f)$ w.r.t. parameters $\mathbf{p}$. In the following, the state values $\mathbf{x}(t_0)$ and $\mathbf{x}(t_f)$ are abbreviated by $\mathbf{x}_0$ and $\mathbf{x}_{t_f}$ respectively.

3.1. Forward Sensitivity

By deriving the sensitivity $\mathbf{S} = \frac{\partial \mathbf{x}}{\partial \mathbf{p}}$ with respect to time, we obtain the following initial value problem for the forward sensitivity [1]:

$$\dot{\mathbf{S}}(t) = \frac{\partial \mathbf{f}(t)}{\partial \mathbf{x}} \mathbf{S}(t) + \frac{\partial \mathbf{f}(t)}{\partial \mathbf{p}}, \quad \mathbf{S}(t_0) = \frac{\partial \mathbf{x}_0}{\partial \mathbf{p}} \tag{6}$$

The terms $\frac{\partial \mathbf{f}}{\partial \mathbf{x}}$ and $\frac{\partial \mathbf{f}}{\partial \mathbf{p}}$ can be calculated by analytically deriving the model dynamics. The sensitivity $\mathbf{S}$ is then determined by numerical integration of (6). The discretized sensitivity matrix is of size $n_x \times (n_x + n_p) \times n_t$. In the rows of $\mathbf{S}$ the states, which are derived, are given. In the columns, the parameters, with respect to which the sensitivity is calculated, are given, cf. Figure 1. So for each parameter n_x differential equations have to be solved which makes the sensitivity computationally expensive.
Since the first order sensitivity is introduced into the cost function, second order sensitivities with respect to the optimization vector are required. These are provided by the tool FALCON.m, if the first order sensitivities are collocated. For the hybrid method, where states are collocated and sensitivities are shooted, they need to be provided by the user. Details regarding the calculation of second order sensitivities can be found in [12].

3.2. Adjoint

As in [1], for the backward sensitivity or the adjoint method we consider the k-th state $x_k(t_f)$. By augmenting $x_k(t_f)$ with an integral over a product of the adjoint function $\boldsymbol{\lambda}$ and the system dynamics and deriving the resulting sum w.r.t. $\mathbf{p}$ we obtain the final value problem

$$\dot{\boldsymbol{\lambda}}^T(t) = -\boldsymbol{\lambda}^T(t) \frac{\partial \mathbf{f}(t)}{\partial \mathbf{x}}, \quad \boldsymbol{\lambda}^{\boldsymbol{T}}(t_f) = \frac{\partial x_k(t_f)}{\partial \mathbf{x}_{t_f}}. \tag{7}$$

The function $\boldsymbol{\lambda}$ is an auxiliary function and by defining its differential equation and the final value as in (7) the computationally expensive forward sensitivity terms $\mathbf{S}(t)$ with $t > t_0$ are eliminated. By integrating $\dot{\boldsymbol{\lambda}}$ backward in time, we obtain $\boldsymbol{\lambda}(t_0)$. In the special case $\mathbf{p} = \mathbf{x}_0$ considered in this study the initial value $\boldsymbol{\lambda}(t_0)$ represents the sensitivity $\frac{\partial x_k(t_f)}{\partial \mathbf{x}_0}$. The relation to the forward sensitivities is then given by [1, 13]:

$$\boldsymbol{\lambda}(t_0) = \frac{\partial x_k(t_f)}{\partial \mathbf{x}_0} = \mathbf{S}_k(t_f) \tag{8}$$

where $\mathbf{S}_k$ denotes the k-th row of $\mathbf{S}$. The size of the discretized adjoint matrix $\boldsymbol{\lambda}$ is $n_x \times n_t$, cf. Figure 1. So, independent from the number of parameters n_x differential equations are solved. Please note that if sensitivities for more than one state are considered, for each state n_x differential equations are introduced for the adjoint.
Since the adjoint is introduced into the cost function, its gradient with respect to the optimization vector needs to be calculated. For the collocated adjoints the tool FALCON.m provides the gradient. For the hybrid method, where the adjoints are integrated in the cost function by shooting, it needs to be provided by the user. The gradient of the adjoint can be calculated based on the sensitivity differential equation in (6). Therefor, let $\mathbf{f}_\lambda \colon \mathbb{R}^{n_\lambda} \times \mathbb{R}^{n_x} \to \mathbb{R}^{n_\lambda}$ with $\dot{\boldsymbol{\lambda}} = \mathbf{f}_\lambda(\boldsymbol{\lambda}; \mathbf{x})$ be the function describing the adjoint differential equation in (7) and let $\mathbf{z}$ be the optimization vector.
Then the gradient $\mathbf{S}_\lambda = \frac{\partial \boldsymbol{\lambda}}{\partial \mathbf{z}}$ of the adjoint can be determined by solving the final value problem

$$\dot{\mathbf{S}}_\lambda(t) = \frac{\partial \mathbf{f}_\lambda(t)}{\partial \boldsymbol{\lambda}} \mathbf{S}_\lambda(t) + \frac{\partial \mathbf{f}_\lambda(t)}{\partial \mathbf{z}}, \quad \mathbf{S}_\lambda(t_f) = \frac{\partial \boldsymbol{\lambda}_{t_f}}{\partial \mathbf{z}}. \tag{9}$$

©2020

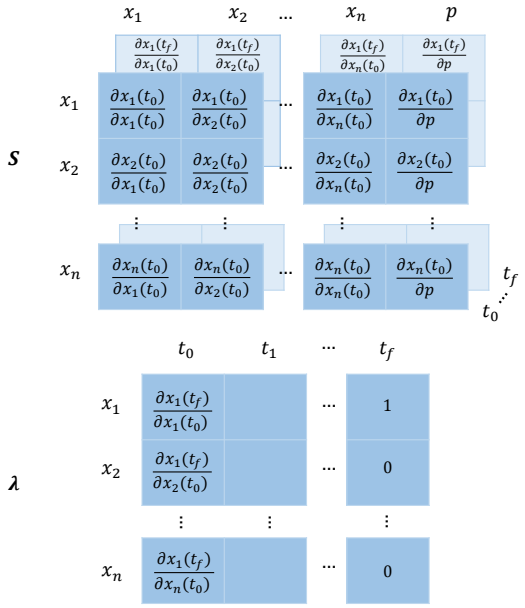

FIGURE 1. Structures of the forward sensitivity matrix $\mathbf{S}$ (top) and adjoint matrix $\boldsymbol{\lambda}$ (bottom) for the special case $\mathbf{p} = \mathbf{x}_0$.

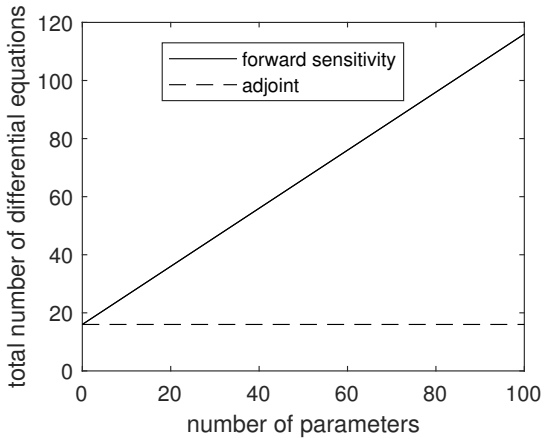

FIGURE 2. Growth of the total number of differential equations for eight states in the robust optimal control problem dependent on the number of parameters for the collocated forward sensitivity and adjoint method. In case of the forward sensitivity method, the problem size increases linearly in n_p whereas it is constant for the adjoint method, if the sensitivity of only one state is considered.

3.3. Comparison and Implementation

Analytically, when calculating a certain sensitivity $\frac{\partial x_k(t_f)}{\partial \mathbf{p}}$, both the forward sensitivity and the adjoint method deliver the same result as stated in [1]. With the forward sensitivities we obtain sensitivities on the whole time interval, so we obtain $\frac{\partial x_k(t)}{\partial \mathbf{p}}$ for all $t \in [t_0, t_f]$. But due to the fact that for each parameter a set of n_x differential equations has to be solved, forward sensitivity calculation comes along with higher computational effort. In contrast, for the adjoint sensitivities, only n_x differential equations for all parameters are solved which is more advantageous especially for a high number of parameters.

When introducing either the forward sensitivity $\mathbf{S}$ or the adjoint $\boldsymbol{\lambda}$ into an optimal control problem we consider two different methods. Since the discretization method for the states is chosen to be the collocation method as stated in section 2, also collocating $\mathbf{S}$ and $\boldsymbol{\lambda}$ might be suitable [8]. Therewith, both the states and the sensitivities are integrated with the same method. As the sensitivities are treated as states, the number of states increases to $2n_x + n_p$ for the forward sensitivity method and to $2n_x$ for the adjoint method. In general, the problem size, i.e. the number of states and constraints, increases in this incorporation method since states and hence constraints are added to the original problem. Especially for the forward sensitivities the problem size increases linearly in n_p.

On the other hand, the problem sparsity in the collocation method is higher in contrast to the shooting method [16]. Figure 2 depicts an example of the growth of the total number of differential equations with the number of parameters for both the forward sensitivity and the adjoint method for $n_x = 8$ states.

Another approach is combining collocation and shooting methods, i.e. the system states are collocated and the sensitivities are shooted in the cost function. The cost function is provided with the discretized states, controls, parameters and time grid, which are used for the single shooting trapezoidal integration of the sensitivities. The output of this cost function is the required sensitivity and its gradient w.r.t. the optimization vector. [12] By this, the problem size does not increase but the problem structure is dense. An overview of the applied combinations is given in Table 1.

3.4. Sensitivity Penalty

In order to calculate robust optimal solutions, we follow the approach of penalizing the cost function for high sensitivities of interest. Let

$$S_{k,i}(t_f) = \frac{\partial x_k}{\partial p_i}(t_f) \tag{10}$$

be the sensitivity of the k-th state w.r.t. the parameter p_i. In the sensitivity penalty approach, not only the nominal Mayer cost function is minimized but the sum of it and

TAB. 1. Overview of methods and problem sizes.

	Number of collocated states	Number of internally integrated states
Collocated Forward Sensitivity	$2n_x + n_p$	0
Collocated Adjoint	$2n_x$	0
Shooted Forward Sensitivity	n_x	$n_x + n_p$
Shooted Adjoint	n_x	n_x

the weighted squared sensitivities, i.e.

$$e(\mathbf{x}(t_0), \mathbf{x}(t_f)) + \sum_{k=1}^{n_x} \sum_{i=1}^{n_p} a_{k,i} \cdot S_{k,i}(t_f)^2 \tag{11}$$

is minimized. With the help of the non-negative weights $a_{k,i}$ this cost function can either be weakly or strongly penalized by sensitivities. The greater $a_{k,i}$ the higher the penalty and the higher the robustness of the solution. On the other hand, the smaller $a_{k,i}$ the less the according sensitivity's influence on the cost function and hence the lower the robustness of the solution. Assuming that the nominal solution is strictly global and unique and the sensitivity $S_{k,i}$ is not zero, the robust solution cannot deliver a smaller nominal Mayer cost function value, since the penalty terms are added and also minimized.

4. MODELLING

In this section, the models for the dynamic system of the Apollo capsule (cf. Figure 3) including the equations of motion, the aerodynamics, atmosphere and thermodynamics are presented. The mass of the Apollo capsule is $m = 5900\text{kg}$ and has a nose radius of $R_n = 4.595\text{m}$. The reference area for the determination of the lift and drag of the shield is $S_{ref} = 12.8794\text{m}^2$.

Equations of Motion

The system is assumed to be a point mass model as in [18]. Positional state and velocity dynamics are described dependent on the angle of attack α and the bank angle μ.

Lift and Drag Coefficient

The lift and drag coefficients C_L and C_D for the capsule are modelled based on Newtonian impact theory in hypersonic regions as a function of the angle of attack α as in [19]:

$$C_L = C_y \cos(\alpha) - C_x \sin(\alpha) \tag{12}$$

$$C_D = C_y \sin(\alpha) + C_x \cos(\alpha) \tag{13}$$

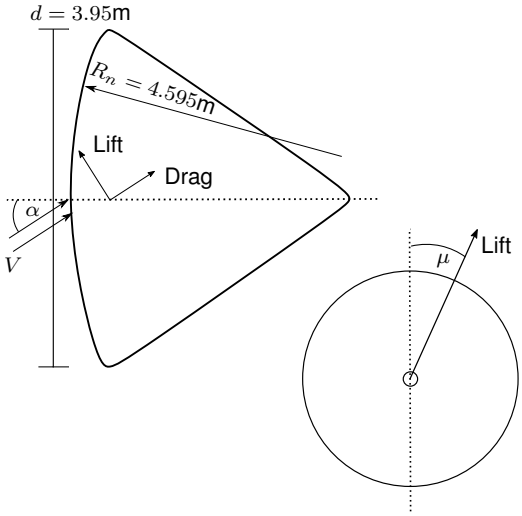

FIGURE 3. Apollo capsule geometry [4, 17].

with the axial and normal force coefficients

$$C_x = \frac{2}{3}\sin(\theta)^3(\sin(\alpha)^2 - \cos(\alpha)^2) + 2\cos(\alpha)^2\sin(\theta) \tag{14}$$

$$C_y = \frac{4}{3}\cos(\alpha)\sin(\alpha)\sin(\theta)^3 \tag{15}$$

where $\theta = 32.055°$ is the cone angle.

Air Density

The model of the air density ρ is an approximation of the U.S. Standard Atmosphere 1976 [3] and describes the air density as a function of the altitude up to 200km. It is represented by an exponential function as follows [18]:

$$\rho(h) = \exp\left(\frac{c_1h^5 + c_2h^4 + c_3h^3 + c_4h^2 + c_5h + c_6}{c_7h^3 + c_8h^2 + c_9h + c_{10}} + \cos(d_1h^{d_2} + d_3)\frac{d_4}{d_5h + d_6} - e_1\exp\left(e_2(h - e_3)^2\right)\right) \tag{16}$$

For the coefficients $c_{1,\ldots,10}, d_{1,\ldots,6}, e_{1,\ldots,3}$ please refer to Table 2.

TAB. 2. Coefficients for density model.

$c_1 = 1.53225 \cdot 10^{-10}$	$d_1 = 2.6294 \cdot 10^{-1}$
$c_2 = -2.13594 \cdot 10^{-8}$	$d_2 = 0.83$
$c_3 = -2.81202 \cdot 10^{-5}$	$d_3 = 3.7$
$c_4 = 6.06600 \cdot 10^{-3}$	$d_4 = 1.0 \cdot 10^{-1}$
$c_5 = -3.46014 \cdot 10^{-1}$	$d_5 = 1.5 \cdot 10^{-2}$
$c_6 = 1.03970$	$d_6 = 3.0 \cdot 10^{-1}$
$c_7 = 0.0$	
$c_8 = 1.76969 \cdot 10^{-4}$	$e_1 = -2.6 \cdot 10^{-1}$
$c_9 = -3.80665 \cdot 10^{-2}$	$e_2 = -5.0 \cdot 10^{-3}$
$c_{10} = 2.15211$	$e_3 = -92.0$

Thermal Model

The heat flux $\dot{q}$ at the stagnation point of the capsule is calculated as in [10] by

$$\dot{q}(t) = K_e \sqrt{\frac{\rho(h(t))}{R_n}} V(t)^3, \tag{17}$$

where $K_e = 5.199111 \times 10^{-5}$ (kg/m^2)$^{1/2}$ is an atmosphere specific constant and R_n is the nose radius of the vehicle.

5. APPLICATION TO REENTRY TRAJECTORIES

In this section, the reentry trajectory of an Apollo capsule is optimized. First, the nominal problem without uncertainties is solved and simulated under parameter perturbations. Afterwards, high sensitivities are penalized as described in section 3. In detail, the sensitivity of the final velocity with respect to initial altitude and flight path angle is reduced. Finally, the results are compared and discussed.

5.1. Nominal Optimization Results

In the nominal optimization the aim is to minimize the heat load at the stagnation point after reentry, hence

$$\min_{\mathbf{x},\mathbf{u}} q(t_f)$$

by finding optimal controls $\alpha \in [-21, 21]$ deg as well as $\mu \in [-30, 30]$deg. Furthermore, the rate of α is constrained to be in the interval $[-2, 2]$deg /s. Initial and final boundary conditions are given in Table 3.
In this setting, the reentry starts in the lower earth orbit at an altitude of 120km. The optimal trajectory is determined for a flight until an altitude of 30km and a velocity of 1.735km/s is reached. The final value for the velocity is chosen to be the final optimal velocity from a previous optimization step without the final boundary for the state V. Since we are interested in the variation of the final velocity w.r.t. the initial altitude and flight path angle it is chosen to be a final boundary condition in the nominal and robust optimization to be able to compare the results. Furthermore, a path constraint on the load factor $\frac{-D}{mg_h}$ is imposed by the lower bound of -5. Here, D is the drag and g_h the gravitational acceleration dependent on altitude.

TAB. 3. Initial and final boundaries. A dash (-) indicates that no constraints are enforced.

State	Symbol	Unit	t_0	t_f
Altitude	h	[km]	120	30
Velocity	V	[km/s]	7.7	1.735
Flight path angle	γ	[deg]	-3	-
Course angle	χ	[deg]	-	-
Longitude	λ	[deg]	-	-
Latitude	ϕ	[deg]	-	-
Heat load	q	[kJ/m^2]	0	-

In Figure 4 the optimal trajectories of the velocity, altitude, flight path angle and heat load together with the corresponding optimal controls α and μ are presented.
It is beneficial to fly with a flight path angle close to the initial flight path angle in the upper layers of the atmosphere. In this region the velocity is close to constant and the heat load increases quickly. At an altitude of around 50km, where the air starts to become denser, the flight path angle decreases in order to use air resistance to reduce velocity and hence to reduce the growth of the heat load. Here, the heat load $q(t_f)$ is 8246.62 kJ/m^2.
Perturbations in the initial altitude and flight path angle might occur due to measurement errors that can lead to discrepancies in the real position and attitude and those which are known to the system [4]. High variations in the final velocity make the landing phase unpredictable and might lead to an unsafe landing. Hence, we investigate the variation of the final velocity with respect to the initial altitude and flight path angle. The perturbations of the initial altitude and flight path angle are assumed to happen up to 1%, hence

$$\tilde{h}_0 = h_0(1 + p_h), \quad p_h \in [-0.01, 0.01], \tag{18}$$

$$\tilde{\gamma}_0 = \gamma_0(1 + p_\gamma), \quad p_\gamma \in [-0.01, 0.01]. \tag{19}$$

In the simulation in Figure 5, we can see that for variations of the initial altitude and the flight path angle the final velocity varies up to 563.5 km/s, which is 32.45%. The sensitivities in this case are $\frac{\partial V(t_f)}{\partial h_0} = 0.27447$ and $\frac{\partial V(t_f)}{\partial \gamma_0} = 361.4493$.

©2020

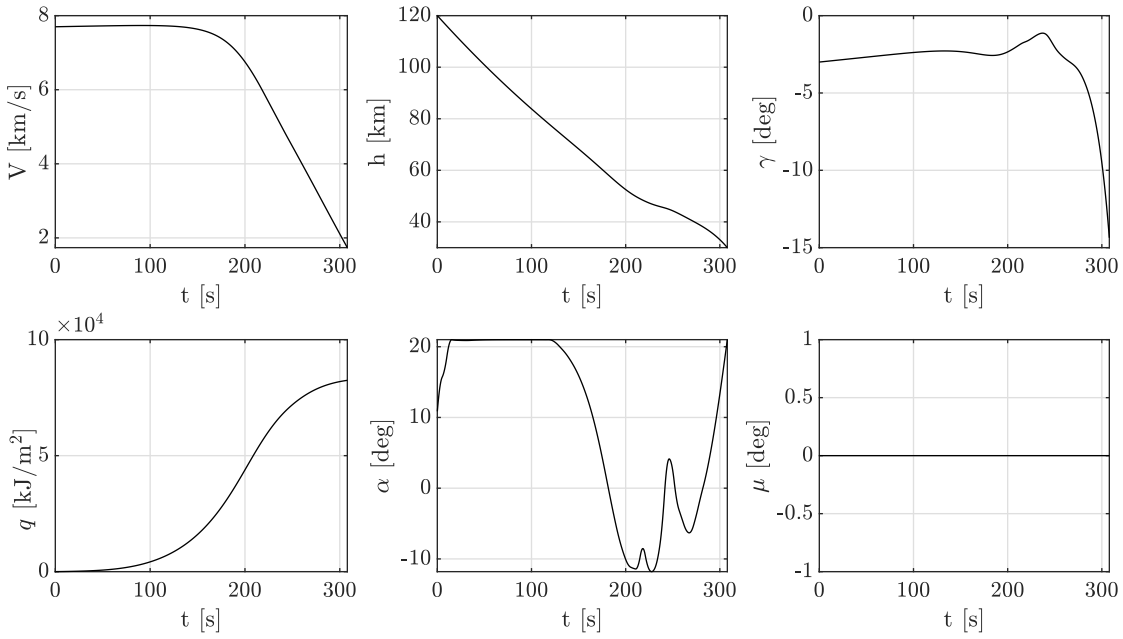

FIGURE 4. Nominal optimal trajectories for velocity V, altitude h, flight path angle γ, heat load q and controls α and μ.

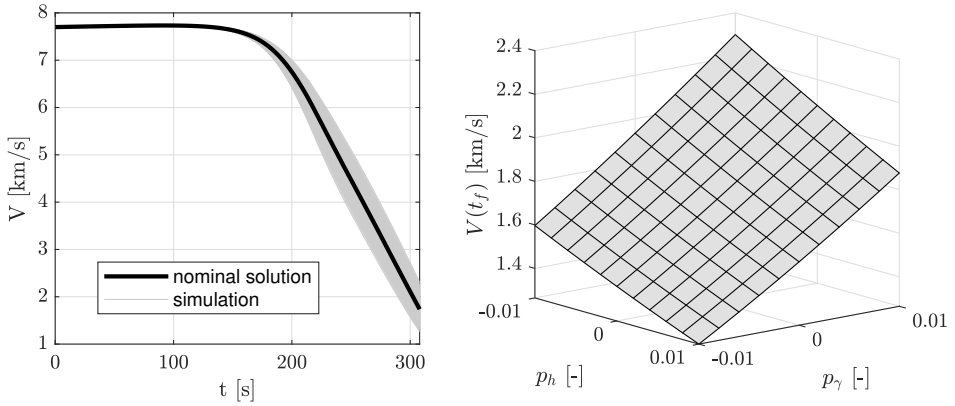

FIGURE 5. Simulation of the velocity history with nominal optimal controls for variations of initial altitude and flight path angle up to 1%.

5.2. Robust Optimization Results

In order to reduce the variations in the final velocity dependent on the initial altitude and flight path angle, a robust trajectory via sensitivity penalty as described in section 3 is conducted. The cost function to be minimized now is

$$\min_{\mathbf{x},\mathbf{u}} q(t_f) + a_1 \left(\frac{\partial V(t_f)}{\partial h_0} \right)^2 + a_2 \left(\frac{\partial V(t_f)}{\partial \gamma_0} \right)^2 \tag{20}$$

with the weights $a_1 = 3{\cdot}10^4$ and $a_2 = 3{\cdot}10^{-3}$. Therefore, four different methods are utilized:

- collocated forward sensitivities
- collocated adjoints
- shooted forward sensitivities
- shooted adjoints

The robust trajectories are presented in Figure 6. At the beginning of the reentry, the nominal and the robust trajectories are similar until an altitude of around 75km. Then, in the robust trajectory the flight path becomes smaller in magnitude in order to reduce altitude more slowly. Furthermore, the velocity is reduced more slowly than in the nominal solution. The final heat load is 9237.96kJ/m^2 which is a rise of 12.02% in contrast to the nominal solution.
In the simulated trajectories in Figure 7, we can see that

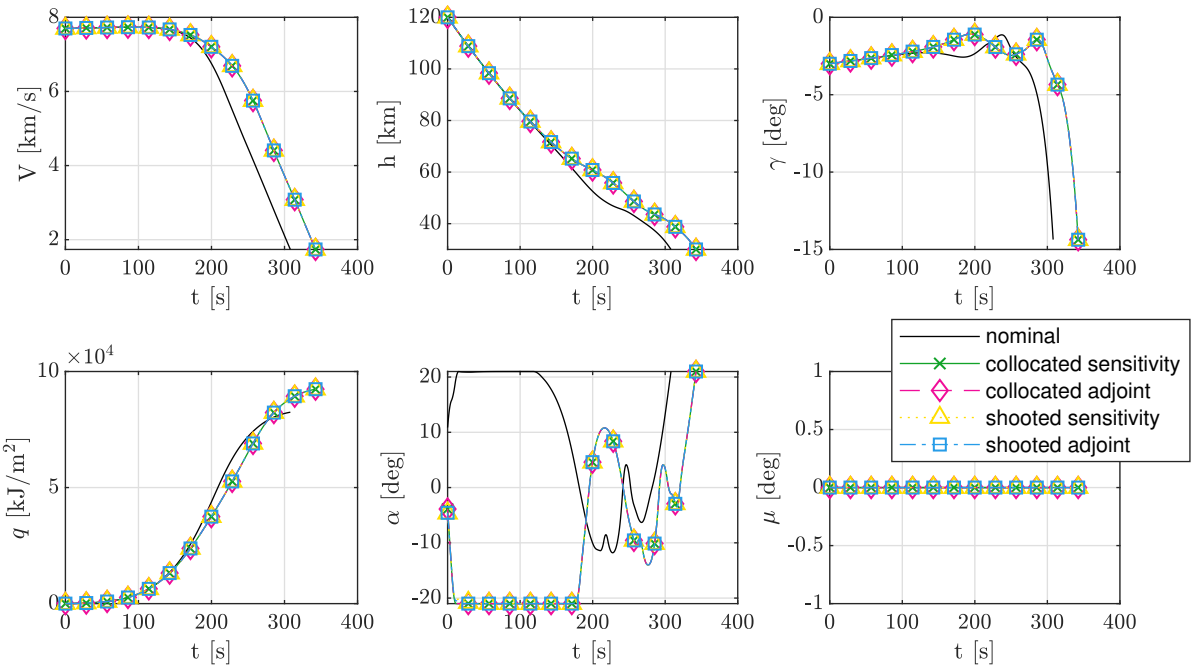

FIGURE 6. Robust optimal trajectories for velocity V, altitude h, flight path angle γ, heat load q and controls α and μ.

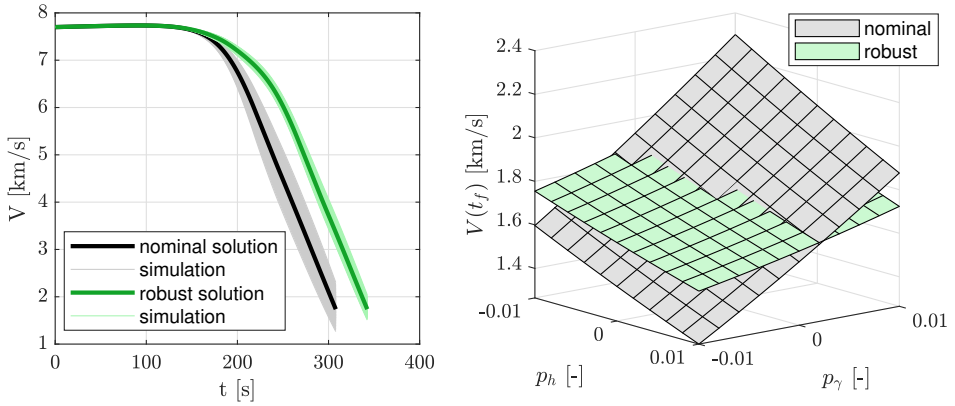

FIGURE 7. Simulation of the velocity trajectory with nominal and robust optimal controls for variation of initial altitude and flight path angle up to 1%. The robust optimal controls reduce the variation in the final velocity.

with the robust controls the variation in $V(t_f)$ for different values of h_0 and γ_0 is less than with the nominal controls. The final velocity now varies up to 302.5km/s, which is 17.42%. Also, the sensitivity values are reduced to $\frac{\partial V(t_f)}{\partial h_0} = 0.10328$ and $\frac{\partial V(t_f)}{\partial \gamma_0} = 266.8226$. The reduction of the sensitivities can also be observed in Figure 8. Please note that the final values of the forward sensitivities equal the initial values of the according adjoints as stated in (8). The cost function and sensitivity values for each method are collected in Table 4.

Together with Figure 6 we can deduce that all four methods, collocated forward sensitivities and adjoints as well as forward sensitivities and adjoints by single shooting, deliver the same solution except for a small discrepancy in the first 10s to 55s in the angle of attack between the collocated and both the shooted forward sensitivities and adjoints. This can be explained by the fact that the system dynamics have to be fulfilled in order to determine their sensitivities. Generally, this is not the case at the beginning of the optimization. Analytically, both the forward sensitivity and adjoint method should deliver the same solution since they both represent the same sensitivity. However, for gradient based methods, it should be noted that the forward sensitivity method might lead

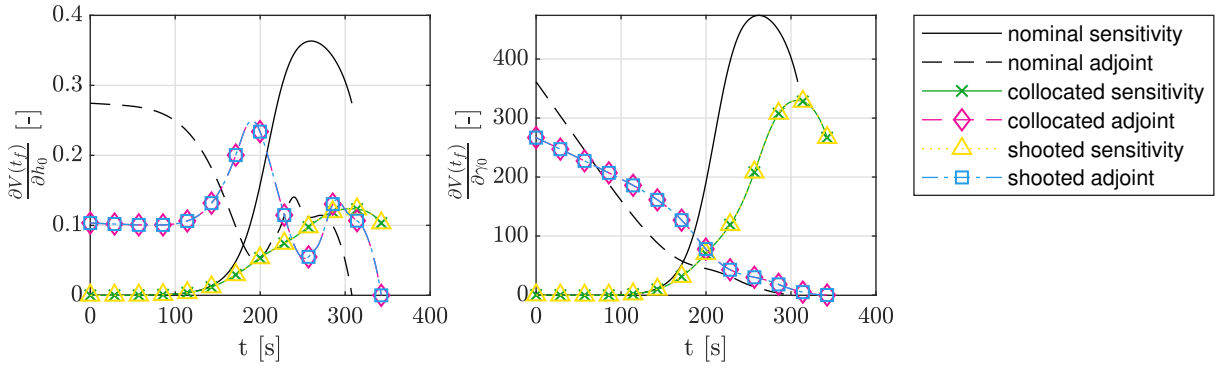

FIGURE 8. Forward sensitivities and adjoints over time.

TAB. 4. Nominal cost function values for $q(t_f)$ and sensitivity values for all methods.

	$q(t_f)$ [kJ/m^2]	$\frac{\partial V(t_f)}{\partial h_0}$	$\frac{\partial V(t_f)}{\partial \gamma_0}$
Nominal	8246.4	0.27447	361.4493
Collocated Sensitivity	9237.9581	0.10328	266.8226
Collocated Adjoint	9237.8828	0.10329	266.8222
Shooted Sensitivity	9238.02	0.10328	266.8085
Shooted Adjoint	9237.7887	0.1033	266.8351

to another local optimum than the adjoint method, since they both are based on different differential equations and hence result in different gradients.

6. CONCLUSION AND OUTLOOK

In this study a robust reentry trajectory of an Apollo capsule is calculated with respect to minimal heating at the stagnation point. Therefore, optimal control methods based on full discretization and trapezoidal integration are used. The robust optimal control method is based on the introduction of a sensitivity penalty where sensitivities of states with respect to uncertain parameters are minimized together with the nominal cost function. Two different methods to calculate the sensitivities are compared, namely the forward sensitivity and the adjoint method. For each method, the sensitivities are incorporated into the optimal control problem first by collocation and second by a hybrid method combining collocation for states and shooting for sensitivities. The resulting robust trajectories give rise to a reentry, where the variance in the velocity after reentry and before the landing phase is reduced when the assumed initial altitude and flight path angle are perturbed. The four methods deliver the same results for sensitivity evaluation and for robust optimal control. For this illustrative example, the adjoint method has shown to be more efficient than the forward sensitivity method, especially together with the collocation method. Further research could be targeted towards an extended adjoint method, where sensitivities via adjoints are calculated for the whole time grid. Also, a problem with a larger set of parameters could be investigated for the hybrid method in order to determine the limitation of the collocated adjoints and the benefit of shooted adjoints. Furthermore, the performance of the forward sensitivity and adjoint method for the determination of sensitivities for multiple states could be studied.

7. CONTACT

tugba.akman@tum.de

8. ACKNOWLEDGEMENTS

This research is supported by Munich Aerospace e.V. in the framework of the project "Reentry Optimization to Minimize Heating or Infrared Signature". Rubens Afonso acknowledges CAPES (grant 88881.145490/2017-01) and the German Ministry of Education and Research through the Alexander von Humboldt Foundation for his fellowship.

9. REFERENCES

[1] M. Gerdts. *Optimal control of ODEs and DAEs*. DeGruyter, Berlin/Boston, 2011.

[2] J. T. Betts. *Practical Methods for Optimal Con-*

trol and Estimation Using Nonlinear Programming. Society for Industrial and Applied Mathematics, Philadelphia, 2010.

[3] US Standard Atmosphere. *US standard atmosphere*. National Oceanic and Atmospheric Administration, Washington, D.C., 1976.

[4] C. A Graves. *Apollo experience report: Mission planning for Apollo entry*. National Aeronautics and Space Administration, Washington, D.C., 1972.

[5] A. Shapiro, D. Dentcheva, and A. Ruszczyński. *Lectures on stochastic programming*. Society for Industrial and Applied Mathematics, Philadelphia, 2009.

[6] D. Xiu. Fast numerical methods for stochastic collocation: A review. *Communications in Computation Physics*, 5(2–4):242–272, 2008.

[7] O. Stein. How to solve a semi infinite optimization problem. *European Journal of Operational Research*, 223(2):312–320, 2012.

[8] R. Loxton, K. L. Teo, and V. Rehbock. Robust suboptimal control of nonlinear systems. *Applied Mathematics and Computation*, 217(14): 6566–6576, 2011.

[9] M. H. Breitner and H. J. Pesch. Reentry trajectory optimization under atmospheric uncertainty as a differential game. In *Advances in dynamic games and applications*, pages 70–86. Birkhäuser, Boston, 1994.

[10] F. Pescetelli, E. Minisci, and R. E. Brown. Re-entry trajectory optimization for a SSTO vehicle in the presence of atmospheric uncertainties. *5th European Conference for Aeronautics and Space Sciences, EUCASS*, 2013.

[11] K. Seywald and H. Seywald. Desensitized optimal control. *AIAA Scitech 2019 Forum*, 2019. doi: 10.2514/6.2019-0651.

[12] S. Hosseini, C. Göttlicher, and F. Holzapfel. Optimal input design for flight vehicle system identification via dynamic programming and the direct method for optimal control. *AIAA Scitech 2019 Forum*, page 1319, 2019.

[13] M. Alexem and A. Sandu. Forward and adjoint sensitivity analysis with continuous explicit runge-kutta methods. *Applied Mathematics and Computation*, 208(2):328–346, 2009.

[14] P. Stapor, F. Fröhlich, and J. Hasenauer. Optimization and profile calculation of ODE models using second order adjoint sensitivity analysis. *Bioinformatics (Oxford, England)*, 34(13):i151–i159, 2018. doi: 10.1093/bioinformatics/bty230.

[15] M. Rieck, M. Bittner, B. Grüter, J. Diepolder, and P. Piprek. FALCON.m user guide, 2020. URL `www.falcon-m.com`.

[16] M. Bittner. *Utilization of problem and dynamic characteristics for solving large scale optimal control problems*. Dissertation, Technische Universität München, 2017.

[17] R. Mehta. Numerical computation of heat transfer on reentry capsules at Mach 5. *43rd AIAA Aerospace Sciences Meeting and Exhibit*, page 178, 2005. doi: 10.2514/6.2005-178.

[18] M. Mayrhofer. *Verbesserung der Missionssicherheit eines zukünftigen zweistufigen Raumtransportsystems mittels Flugbahnoptimierung*. Dissertation, Technische Universität München, 2002.

[19] A. Viviani, G. Pezzella, and D. Cinquegrana. Aerothermodynamic analysis of an Apollo-like reentry vehicle. *14th AIAA/AHI Space Planes and Hypersonic Systems and Technologies Conference*, page 8082, 2016. doi: 10.2514/6.2006-8082.

©2020